Acta Crystallographica Section F
Structural Biology and Crystallization Communications
ISSN 1744-3091

Structure of photosynthetic glyceraldehyde-3-phosphate dehydrogenase (isoform A_4) from *Arabidopsis thaliana* in complex with NAD

Simona Fermani,[a] Francesca Sparla,[b] Lucia Marri,[b] Anton Thumiger,[b] Paolo Pupillo,[b] Giuseppe Falini[a]* and Paolo Trost[b]

[a]Department of Chemistry, University of Bologna, Via Selmi 2, 40126 Bologna, Italy, and [b]Department of Experimental Evolutionary Biology, University of Bologna, Via Irnerio 42, 40126 Bologna, Italy

Correspondence e-mail: giuseppe.falini@unibo.it

Received 23 February 2010
Accepted 12 April 2010

PDB Reference: glyceraldehyde-3-phosphate dehydrogenase, 3k2b.

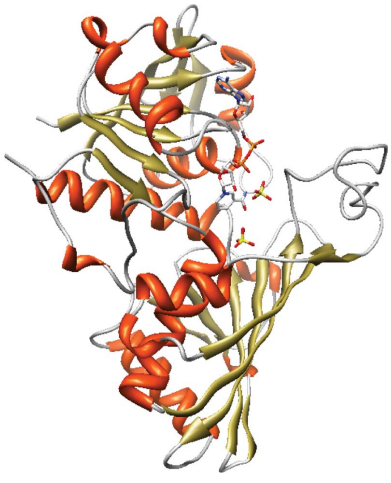

© 2010 International Union of Crystallography
All rights reserved

The crystal structure of the A_4 isoform of photosynthetic glyceraldehyde-3-phosphate dehydrogenase (GAPDH) from *Arabidopsis thaliana*, expressed in recombinant form and complexed with NAD, is reported. The crystals, which were grown in 2.4 *M* ammonium sulfate and 0.1 *M* sodium citrate, belonged to space group *I*222. The asymmetric unit includes ten subunits, *i.e.* two independent tetramers plus a dimer that generates a third tetramer by a crystallographic symmetry operation. The crystal structure was solved by molecular replacement and refined to an *R* factor of 23.7% and an $R_{\rm free}$ factor of 28.9% at 2.6 Å resolution. In the final model, each subunit binds one NAD^+ molecule and two sulfates, which occupy the P_s and the P_i anion-binding sites. Detailed knowledge of this structure is instrumental for structural investigation of supramolecular complexes of A_4-GAPDH, phosphoribulokinase and CP12, which are involved in the regulation of photosynthesis in the model plant *A. thaliana*.

1. Introduction

Oxygen-photosynthetic organisms contain both glycolytic and photosynthetic isozymes of glyceraldehyde-3-phosphate dehydrogenase (GAPDH), all of which are evolutionarily related and show highly conserved amino-acid sequences (Figge *et al.*, 1999). Glycolytic GAPDH isozymes are characterized by absolute specificity for NAD and generally lack evident regulatory mechanisms. Photosynthetic GAPDH isozymes catalyze the single reducing step of the Calvin cycle for CO_2 fixation and can use both NADPH and NADH as coenzymes, although NADPH is the preferred coenzyme. In contrast to glycolytic GAPDH, photosynthetic GAPDH isozymes are finely regulated in a complex manner that involves the formation of supramolecular aggregates (Trost *et al.*, 2006).

Most photosynthetic eukaryotes, as well as cyanobacteria, possess a photosynthetic GAPDH made up of four *A* subunits (Cerff, 1979; Ferri *et al.*, 1990; Tamoi *et al.*, 1996; Koksharova *et al.*, 1998; Scagliarini *et al.*, 1998; Graciet, Lebreton *et al.*, 2003). In addition to this A_4 isoform, land plants contain further isoforms made up of *A* and *B* subunits in stoichiometric ratios (A_2B_2 and A_8B_8; Pupillo & Giuliani Piccari, 1975; Petersen *et al.*, 2006). The *A* and *B* subunits are very similar in sequence, although the *B* subunits include an exclusive C-terminal extension that is absent from the *A* subunits. Thanks to the C-terminal extension of the *B* subunits, the heteromeric isoforms (A_2B_2, A_8B_8) are mutually interconvertible and are autonomously regulated by thioredoxins, pyridine nucleotides, ATP and the GAPDH substrate 1,3-bisphosphoglycerate (Pupillo & Giuliani Piccari, 1975; Trost *et al.*, 1993; Baalmann *et al.*, 1996; Sparla *et al.*, 2005).

Homotetrameric GAPDH (A_4 isoform) is not regulated in the same way because it lacks the C-terminal extension of the *B* subunits. Nevertheless, regulation of A_4-GAPDH is achieved *in vivo* by the action of the scaffold protein CP12 (Wedel & Soll, 1998; Graciet, Gans *et al.*, 2003; Trost *et al.*, 2006). Under the oxidizing conditions that prevail in chloroplasts in the dark, two internal disulfide bonds are formed in CP12. Oxidized CP12 can bind A_4-GAPDH complexed with NAD and then recruit phosphoribulokinase (PRK), which catalyzes one of the two ATP-dependent reactions of the Calvin cycle

(Graciet, Gans *et al.*, 2003; Marri *et al.*, 2005). The final GAPDH–CP12–PRK complex includes two tetramers of GAPDH and two dimers of PRK interlinked by four monomers of CP12 (Marri *et al.*, 2008). Enzymes embedded in the complex are strongly inhibited, but can recover full activity upon dissociation. Release of active GAPDH and PRK from the complex occurs *in vivo* in the light and is promoted by reduced thioredoxins, NADP(H), ATP and 1,3-bisphosphoglycerate (Scheibe *et al.*, 2002; Graciet *et al.*, 2004; Marri *et al.*, 2005, 2009; Howard *et al.*, 2008). Both autonomous regulation of *AB*-GAPDH isoforms and CP12-dependent regulation of A_4-GAPDH coexist in chloroplasts of land plants and contribute to the essential coordination between carbon metabolism and the light-dependent reactions of photosynthesis (Scheibe *et al.*, 2002; Trost *et al.*, 2006; Howard *et al.*, 2008).

To date, crystal structures of photosynthetic GAPDH isoforms have only been solved for a higher plant (*Spinacia oleracea*) and a cyanobacterium (*Synechococcus* PCC7942). The structure of *Synechococcus* GAPDH was solved in both apo (Kitatani *et al.*, 2006*b*) and holo forms (complexed with NADP; Kitatani *et al.*, 2006*a*). Structures of spinach A_4-GAPDH have been solved in the apo form (Cámara-Artigas *et al.*, 2006) and in complex with either NADP (Sparla *et al.*, 2004) or NAD (Falini *et al.*, 2003). A low-resolution structure of spinach A_2B_2-GAPDH inhibited by the C-terminal extension and in complex with NADP has also been described (Fermani *et al.*, 2007). All of these GAPDH structures are similar, but subtle differences in the catalytic domain and the compactness of the tetramer may explain the markedly different kinetic properties of these isoforms (Falini *et al.*, 2003; Sparla *et al.*, 2004; Cámara-Artigas *et al.*, 2006; Fermani *et al.*, 2007).

With the final goal of solving the crystal structures of supramolecular complexes of A_4-GAPDH with PRK and CP12 reconstituted using recombinant proteins obtained from the model plant *Arabidopsis thaliana* (Marri *et al.*, 2005), we here present the crystal structure at 2.6 Å resolution of recombinant *A. thaliana* A_4-GAPDH in complex with NAD, *i.e.* under appropriate conditions for binding CP12.

2. Material and methods

2.1. Protein-solution preparation

Cloning, heterologous expression and purification of *A. thaliana* A_4-GAPDH was performed as described by Marri *et al.* (2005). For crystallization trials, the recombinant protein was concentrated to 10 mg ml^{-1} in 25 m*M* phosphate buffer pH 7.5 containing 1 m*M* NAD.

2.2. Crystallization and data collection

Initial crystallization experiments were performed by the sitting-drop vapour-diffusion method using commercially available screens in a 24-well VDX plate (Hampton Research). JBScreen Classic Kits 1–10 were used as reservoir solution (750 µl), while the drop was formed of 2 µl protein solution and 2 µl reservoir solution. The plates were stored at 293 K. Crystals suitable for diffraction experiments (main axis of about 150 µm) appeared after two weeks in one condition corresponding to JBScreen 6 D1, which contained 2.4 *M* ammonium sulfate and 0.1 *M* sodium citrate. Crystals were cryoprotected by soaking them in a solution consisting of 2.4 *M* ammonium sulfate, 10%(*v*/*v*) glycerol and 1 m*M* NAD. Data were collected from one crystal on ESRF beamline ID14-1 using a wavelength of 0.934 Å, a sample-to-detector distance of 300 mm and an oscillation angle of 1°. A complete data set was recorded on an ADC Quantum 210 CCD detector to a resolution of 2.6 Å. Diffraction data were processed and scaled using the *DENZO* and *SCALEPACK* programs from the *HKL*-2000 package (Otwinowski & Minor, 1997). The crystal belonged to space group *I*222 and contained two tetramers and one dimer in the asymmetric unit, corresponding to a solvent content of about 60% (Matthews, 1968). The unit-cell parameters and data-collection statistics are shown in Table 1.

Table 1
Unit-cell parameters and data-collection, refinement and geometry statistics for A_4-GAPDH–NAD from *A. thaliana*.

Values in parentheses are for the last resolution shell

Unit-cell parameters and data-collection statistics	
Space group	*I*222
Unit-cell parameters (Å)	a = 150.74, b = 188.63, c = 314.13
Resolution limits (Å)	94.2–2.6 (2.69–2.6)
Measured reflections	775580
Unique reflections	131352
R_{merge} (%)	10.0 (69.7)
Completeness (%)	96.1 (76.4)
$I/\sigma(I)$	12.7 (1.2)
Redundancy	5.9 (3.0)
Refinement and geometry statistics	
No. of protein atoms	25525
No. of water molecules	882
R/R_{free} (%)	23.7/28.9
Mean B (Å^2)	59.80
B (Wilson plot) (Å^2)	40.50
B, protein atoms (Å^2)	60.01
B, solvent atoms (Å^2)	63.38
R.m.s.d. bond lengths (Å)	0.007
R.m.s.d. bond angles (°)	1.30

2.3. Structure solution and refinement

The structure of recombinant A_4-GAPDH from *A. thaliana* was solved by molecular replacement using the coordinates of recombinant A_4-GAPDH from spinach complexed with NAD as a probe (PDB code 1nbo; Falini *et al.*, 2003). The cofactor, sulfate ions and water molecules were not included in the model. Rotation and translation searches performed with the program *AMoRe* (Navaza, 1994) clearly showed the positions of one tetramer and a dimer that formed a tetramer by the twofold crystallographic axis. The third solution was not clear and the position of the second tetramer was determined using the program *EPMR* (Kissinger *et al.*, 2001), fixing the coordinates of the tetramer and dimer determined previously as a partial structure.

Refinement procedures were carried out with the program *CNS* (Brünger *et al.*, 1998) and the model was examined and rebuilt manually with the graphics program *XtalView* (McRee, 1999). Refinement included data in the range 8.0–2.7 Å. A total of 5% of the data were selected randomly for R_{free} calculations. Rigid-body refinement of each structure converged quickly and was followed by simulated-annealing and temperature-factor refinement. After a few cycles of energy minimization and *B*-factor refinement, the electron-density maps unambiguously gave the position of NAD, which was introduced into the model. Two positive electron densities were found in the catalytic domain of each subunit and two sulfate ions were added to the model at locations corresponding to the maxima of the $2F_o - F_c$ electron density. In the final stage of the refinement the solvent network was built: any peak in the $(F_o - F_c)$ maps contoured at 3 Å was identified as a water molecule if favourable interactions were established between this site and the protein. This molecule was conserved in the model if it was contoured at 0.8 Å in the $(2F_o - F_c)$ map calculated in the following refinement cycles. Several sulfate ions from the crystallization solution were positioned at the surface of protein chains using the same criteria as applied to water molecules.

In the final cycle of refinement the resolution was extended to 2.6 Å with a σ cutoff on amplitudes equal to 0. The refinement statistics together with statistics concerning the geometry of the final models are given in Table 1.

The majority of residues (78.6%) lie in the most favoured regions of the Ramachandran plot as defined by *PROCHECK* (Laskowski *et al.*, 1993); the remainder of the residues are in the additional and generously allowed regions. The conserved residue Val237, which was well defined in the $(2F_o - F_c)$ electron density, shows unfavourable dihedral angles as previously observed in native and recombinant spinach A_4-GAPDH (Fermani *et al.*, 2001; Sparla *et al.*, 2004). The estimated coordinate error in the atomic positions obtained from the

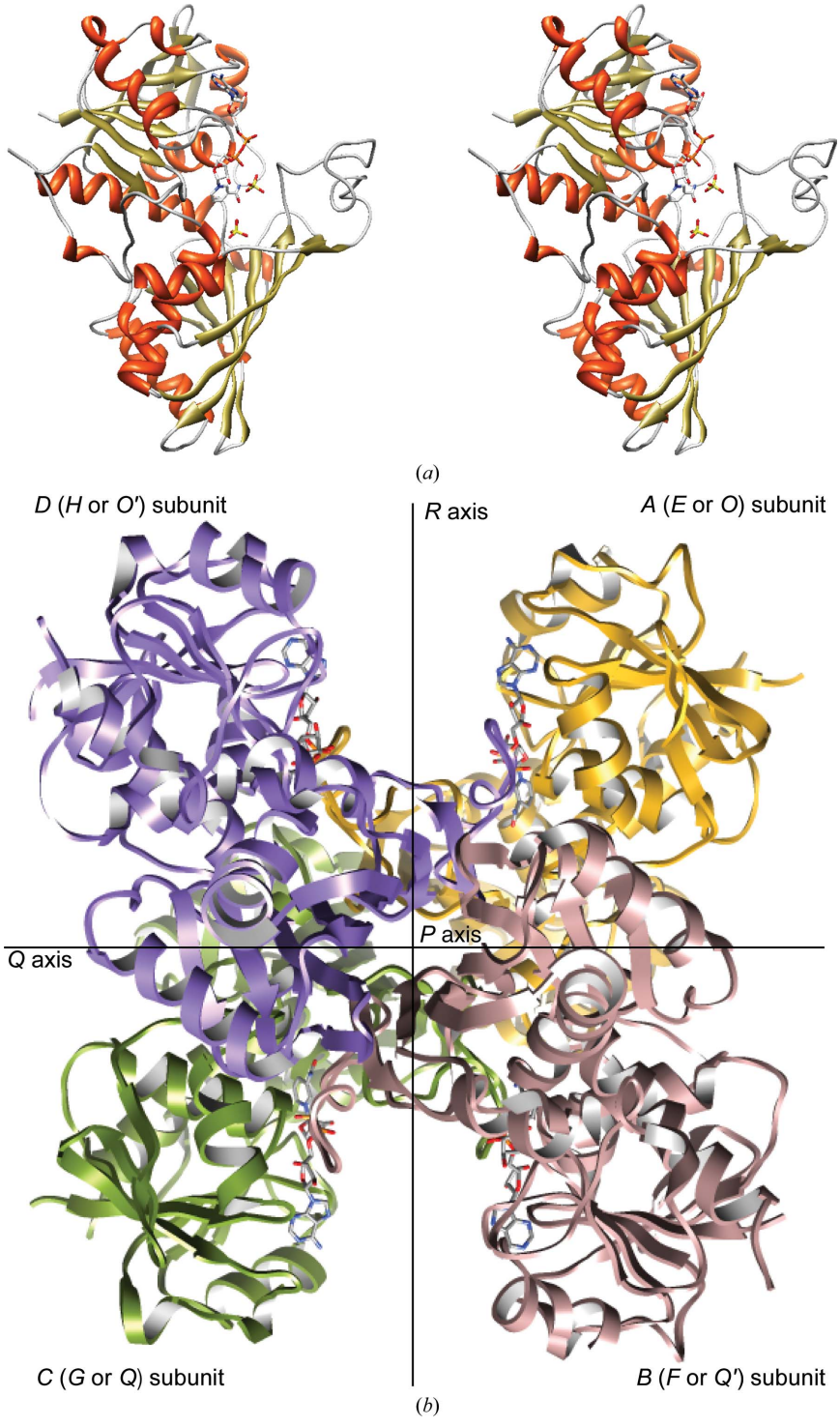

Figure 1
(*a*) Cross-eyed stereoview of the fold of subunit *O* of recombinant A_4-GAPDH complexed with NAD from *A. thaliana*, in which secondary-structure regions are highlighted in different colours. (*b*) Structure of the *ABCD* tetramer of recombinant A_4-GAPDH–NAD from *A. thaliana*; the sulfate ions are not shown. The corresponding subunits of the other two tetramers are indicated in parentheses. These images were produced using *Chimera* (Pettersen *et al.*, 2004).

Luzzati plot (Luzzati, 1952) was 0.39 Å. The coordinates of the structure of recombinant A_4-GAPDH from *A. thaliana* have been deposited in the PDB under accession code 3k2b.

3. Results and discussion

3.1. Crystal structure of A_4-GAPDH from *A. thaliana* complexed with NAD

The final model of A_4-GAPDH–NAD from *A. thaliana* is made up of ten subunits in the asymmetric unit of space group *I*222. The subunits, which are indicated as *A*, *B*, *C*, *D*, *E*, *F*, *G*, *H*, *O* and *Q*, have been named according to the *Bacillus stearothermophilus* GAPDH (Bieseker *et al.*, 1977) and spinach chloroplast A_4-GAPDH models (Fermani *et al.*, 2001) and the residues have been numbered to maximize the homology between the sequences. In the model, the N- and C-terminal ends of different subunits are slightly different: subunits *O*, *A* and *B* contain residues 0*A*–333, with the first two residues (Ala0*A* and Lys0) being derived from the expression vector used to produce the recombinant protein (Marri *et al.*, 2005), subunits *C*, *D*, *F*, *G* and *Q* contain residues 0–333 because of a lack of electron density corresponding to the first residue Ala0*A*, subunit *E* contains residues 0*A*–332 (there was no electron density associated with the terminal residue Lys333) and subunit *H* contains residues 0–332 (no electron density was associated with residues Ala0*A* and Lys333).

The asymmetric unit includes two tetramers (*ABCD* and *EFGH*) and a dimer *OQ*. A third tetramer with pseudo-222 symmetry, *OQO′Q′*, was generated from the *OQ* dimer using a crystallographic twofold axis. The tetramers *ABCD* and *EFGH* show pseudo-222 noncrystallographic symmetry. Indeed, the three molecular axes of the tetramers (axes *P*, *R* and *Q*) do not correspond to the crystallographic axes, except for the crystallographic axis that generates the *OQO′Q′* tetramer, which is coincident with the molecular axis *R* (Fig. 1).

Although noncrystallographic symmetry restraints were not employed in the final cycles of the refinement process, the conformations of all of the subunits in the final model are quite similar. The superimposition of the backbone atoms of the *O* subunit, which was used as a reference, with each of the other subunits gave root-mean-square deviations ranging from 0.354 Å (*O*/*A*) to 0.588 Å (*O*/*F*). The tetramers also show a similar structural organization, with the root-mean-square deviation on backbone atoms of tetramer pairs being between 0.604 Å (*OQO′Q′*/*ABCD*) and 0.815 Å (*OQO′Q′*/*EFGH*). However, it should be mentioned that the tetramer *EFGH* shows less defined electron density with respect to the other chains of the asymmetric unit.

Each subunit contains one NAD molecule characterized by well defined electron density. The coenzyme is bound to the protein in an extended conformation, as previously observed in the structure of spinach A_4-GAPDH (Falini *et al.*, 2003), and is kept in place by several hydrogen bonds (Fig. 2, Table 2). The adenine and nicotinamide rings are roughly perpendicular to the average planes of the neighbouring riboses. The conformation of the adenine is *syn* and that of the nicotinamide ring is *anti*. The planar adenine is located between the methyl groups of two threonine residues (33 and 96). The orientation of the nicotinamide ring is stabilized by an intramolecular hydrogen bond involving the NAD atoms O1N and N7N and by a hydrophobic interaction with the side chain of Ile11, while a different orientation is sterically hindered by the Tyr311 side chain. Both furanose rings are in the C2′-*endo* conformation. All of the NAD residues assume the same structure in the ten subunits in the asymmetric unit, except for that associated with subunit *E*, in which the adenine and nicotinamide rings are slightly shifted.

Table 2
Interactions involving the NAD molecule in the reference *O* chain.

The shortest contacts (less than 3.5 Å) with protein atoms, sulfate ions and solvent molecules are listed.

		Distance (Å)
NAD N7N	NAD O1N	3.02
NAD O2B	Thr33 OG1	3.15
NAD N6A	Arg77 O	3.17
NAD O2B	Asp32 OD2	2.96
NAD O3B	Asp32 OD2	3.25
NAD O3B	Asp32 OD1	2.55
NAD O3B	Gly9 N	3.42
NAD O2A	Arg10 N	3.09
NAD O2N	Arg10 N	2.89
NAD O2N	Ile11 N	2.87
NAD O7N	Asn313 ND2	2.70
NAD O2D	$SO_4$336 O1	2.83
NAD O2D	$SO_4$336 O4	2.82
NAD O2D	W397	3.26
NAD O3D	W367	3.42
NAD N7N	W346	2.76
NAD O1N	W370	2.83
NAD O2N	W434	2.94
NAD O3	W436	3.18
NAD O1A	W436	2.97
NAD O2A	W359	2.91
NAD O2A	W435	2.66
NAD N7A	W440	2.89

Two sulfate ions derived from the crystallization medium are positioned in the active site of each subunit of *A. thaliana* A_4-GAPDH–NAD. In all chains the sulfate ions are localized in proximity (less than 1 Å apart) of the P_s site and the classic P_i site observed in other GAPDH structures (Table 3), including spinach A_4-GAPDH complexed with NADP (Fermani *et al.*, 2001). Based on detailed studies of glycolytic GAPDHs, P sites have been shown to correspond to binding sites for phosphate groups of glyceraldehyde-

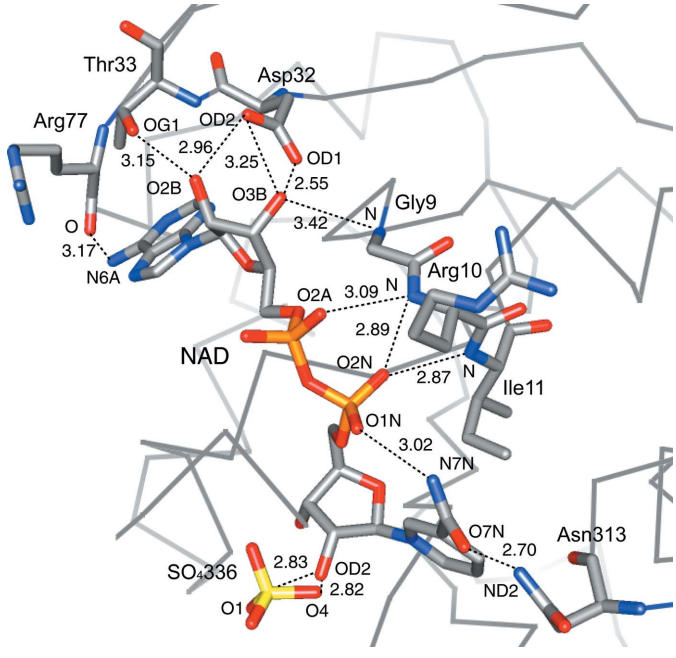

Figure 2
NAD cavity of subunit *O* of recombinant A_4-GAPDH from *A. thaliana*. The NAD, the sulfate ion and the protein-chain residues interacting with NAD are shown in stick representation. The remaining *O*-subunit chain is shown as a wire. The bond interactions are shown as dashed lines. The distance between interacting atoms is reported in Å. The interactions between NAD and water molecules are not shown for clarity but are reported in Table 2. This image was produced using *Chimera* (Pettersen *et al.*, 2004).

3-phosphate, inorganic phosphate and 1,3-bisphosphoglycerate (Moras *et al.*, 1975). A different site named 'new' P_i, about 3 Å away from the classic P_i site, has also been described in several GAPDH structures (Kim *et al.*, 1995) and was found to be occupied by the C3-phosphate of the thioacylenzyme intermediate in *B. stearothermophilus* GAPDH (Moniot *et al.*, 2008) and by that of glyceraldehyde-3-phosphate in the crystal structure of the ternary complex of *Cryptosporidium parvum* GAPDH (Cook *et al.*, 2009). However, it is possible that the classic P_i site is also involved in the complex catalytic mechanism of GAPDH either for binding the C1-phosphate of 1,3-bisphosphoglycerate or for inorganic phosphate binding (Moniot *et al.*, 2008). Although in some subunits of *A. thaliana* A_4-GAPDH–NAD the sulfate ion in the P_i site occupied an intermediate position between the classic and the 'new' P_i sites, this position was generally closer to the classic P_i site than to the 'new' P_i site. Of the ten independent subunits of the model, only subunit *D* contained a sulfate ion that was localized in closer proximity to the 'new' P_i site (Table 3). However, this site always involved the same chemical environment.

The electron-density map clearly shows additional sulfate ions located on the surface of different subunits: one on subunits *D*, *F* and *H*, two on subunits *C* and *E*, three on subunits *B*, *G* and *Q*, four on subunit *O* and five on subunit *A*. These sulfate ions are stabilized by interactions with specific amino-acid side chains and/or the network of water molecules. In all subunits except subunit *Q*, a sulfate ion is stabilized by interaction with the NH1 and NH2 atoms of Arg260. A second common site for superficial sulfate ions is close to residues Ser138 and His139 (subunits *A*–*C*, *G* and *O*). Other sulfate ions interacted with the NE atom of Arg102 (subunits *A*, *B* and *O*), the O atom of Leu216 (subunits *G* and *Q*), the N atom of Ala252 (subunit *A*), the OD1 atom of Asn331 (subunit *E*), the N atom of Thr62 (subunit *O*), the NH1 atom of Arg284 and the N atom of Ala252 (subunit *Q*). In addition, the asymmetric unit contained 882 water molecules.

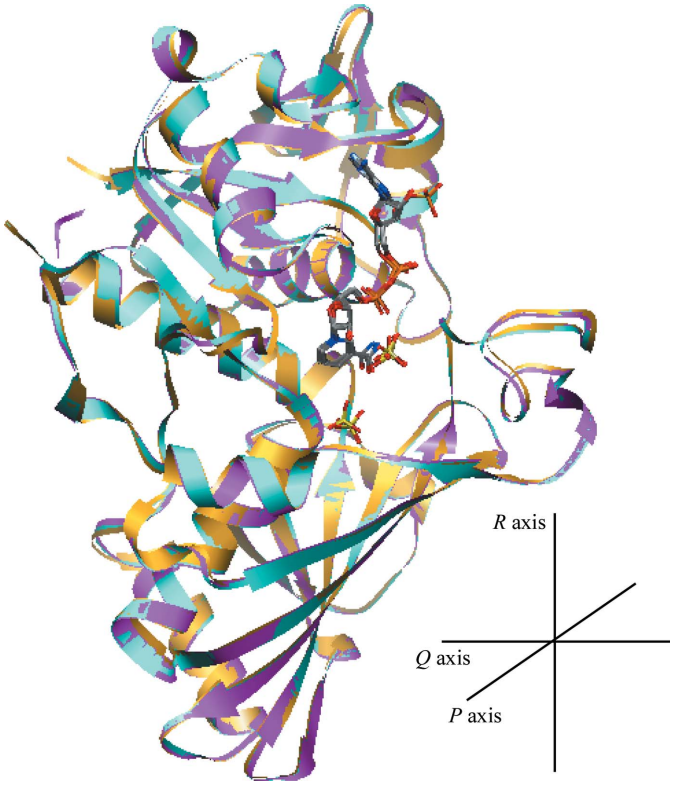

Figure 3
Superimposition of the *O* chain of A_4-GAPDH–NAD from *A. thaliana* (gold) with A_4-GAPDH–NAD from *S. oleracea* (magenta; Falini *et al.*, 2003) and A_4-GAPDH–NADP from *S. oleracea* (cyan; Sparla *et al.*, 2004). This image was produced using *Chimera* (Pettersen *et al.*, 2004).

Table 3
Distances (Å) between sulfate ions (S atoms) cocrystallized in the catalytic site of A_4-GAPDH–NAD from *A. thaliana* ($SO_4$336 and $SO_4$337) and sulfate ions localized in the typical P_s site (subunit *O* of A_4-GAPDH–NAD from *S. oleracea*; Falini *et al.*, 2003), the new P_i site (subunit *O* of A_4-GAPDH–NAD from *S. oleracea*; Falini *et al.*, 2003) and the classic P_i site (subunit *O* of A_4-GAPDH–NADP from *S. oleracea*; Fermani *et al.*, 2001).

Superimpositions were performed by *Chimera* (Pettersen *et al.*, 2004).

A. thaliana A_4-GAPDH–NAD subunit	Sulfate ion	Distance from P_s site (Å)	Sulfate ion	Distance from new P_i site (Å)	Distance from classic P_i site (Å)
A	$SO_4$336	0.46	$SO_4$337	2.54	0.27
B		0.88		2.60	0.36
C		0.25		2.51	0.19
D		0.95		0.36	2.52
E		0.54		2.37	0.42
F		0.96		1.94	0.47
G		0.89		3.06	1.07
H		0.38		2.17	0.40
O		0.60		1.78	0.85
Q		0.32		2.38	0.22

3.2. Comparison between A_4-GAPDH–NAD from *A. thaliana* and *S. oleracea*

The amino-acid sequences of GAPDH subunit *A* from *A. thaliana* and from *S. oleracea* are 87.5% identical. Only a few amino acids are mutated and they appear not to be crucial for the catalytic activity of the enzyme. The reference *O* subunit of A_4-GAPDH–NAD from *A. thaliana* shows high structural similarity to the *O* subunit of the A_4-GAPDH–NAD (Falini *et al.*, 2003) and A_4-GAPDH–NADP (Sparla *et al.*, 2004) structures from *S. oleracea*, giving root-mean-square deviations on backbone atoms of 0.334 and 0.341 Å, respectively (Fig. 3). The overall organization of the A_4-GAPDH–NAD tetramers is also similar: superimposition of the backbone atoms of the *OQO′Q′* tetramer from *A. thaliana*, chosen as a reference, and the *OPQR* tetramer from *S. oleracea* (Falini *et al.*, 2003) gave a root-mean-square deviation of 0.587 Å.

A difference between the two structures is found in the location of the sulfate ion within the P_i site. While in *A. thaliana* A_4-GAPDH–NAD this sulfate ion is generally in the proximity of the classic P_i site, in spinach A_4-GAPDH complexed with the same coenzyme (NAD) sulfate ions occupied the 'new' P_i site or an intermediate position between the 'new' and classic P_i sites (Falini *et al.*, 2003; Table 3, Fig. 4*a*).

Interestingly, Ala200 in *A. thaliana* GAPDH subunit *A* is substituted by Cys200 in *S. oleracea* GAPDH subunit *A*, which forms an inter-chain disulfide bridge (Fermani *et al.*, 2001; Falini *et al.*, 2003). The absence of the inter-chain disulfide bridge does not influence the general packing in the tetramer, although the Cys200Ala mutation causes the unfolding of a short helix (199–201) in the *A. thaliana* protein which is associated with a reduction in the distance (0.54 Å) between the C^{α} atoms of the facing residues 200 (Fig. 4*b*).

4. Concluding remarks

The overall structure of photosynthetic A_4-GAPDH complexed with NAD from *A. thaliana* is similar to that previously reported from *S. oleracea* (Falini *et al.*, 2003). In particular, the coenzyme NAD is

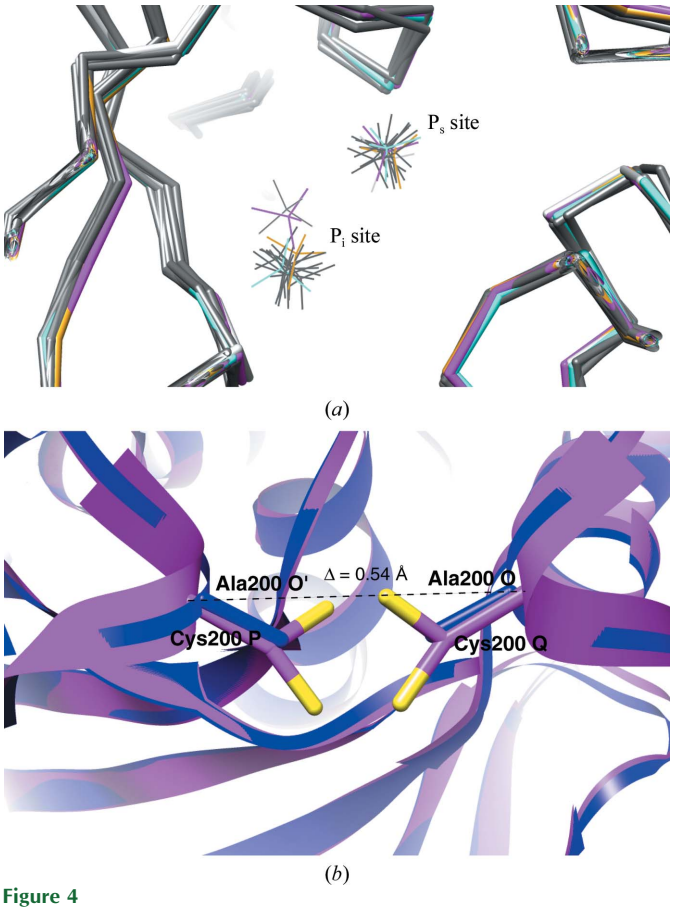

Figure 4
(*a*) Superimposition of the sulfate ions in the P_s and P_i sites from the structure of A_4-GAPDH–NAD from *A. thaliana* (the *O* subunit in shown in gold and the other subunits are shown in grey) and from A_4-GAPDH–NAD (magenta; 'new' P_i site; Falini *et al.*, 2003) and A_4-GAPDH–NADP (cyan; classic P_i site; Fermani *et al.*, 2001) from *S. oleracea*. (*b*) Superimposition of the tetramer *OQO′Q′* from the *A. thaliana* structure (blue) and of the *OPQR* tetramer from the *S. oleracea* A_4-GAPDH–NAD structure (magenta; Falini *et al.*, 2003). Residue 200 is shown: it is an Ala in *A. thaliana* and a Cys in *S. oleracea*, where it assumes a double conformation. The mutation Cys200Ala produces a reduction in the distance between the C^{α} atoms of the facing residues of 0.54 Å. These images were produced using *Chimera* (Pettersen *et al.*, 2004).

bound to the protein in the same way and the subunits show a very similar folding. The occupation of P_s sites by sulfate ions is also similar, while occupation of the P_i site mainly corresponds to the classic position in the *A. thaliana* protein and differs from the 'new' position observed in spinach A_4-GAPDH complexed with the same coenzyme. Owing to the substitution of Cys200 (spinach) by Ala200 in the sequence of *A. thaliana* GAPDH subunit *A*, no inter-chain disulfide bridges are present in the *A. thaliana* tetramer.

This work was financed by the Italian Ministry of Universities (grants FIRB and PRIN). The European Synchrotron Radiation Facility (Grenoble, France) is gratefully acknowledged for access to synchrotron facilities. GF and SF thank the Consorzio Interuniversitario di Ricerca per la Chimica dei Metalli nei Sistemi Biologici for support.

References

Baalmann, E., Scheibe, R., Cerff, R. & Martin, W. (1996). *Plant Mol. Biol.* **32**, 505–513.
Bieseker, G., Harris, J. I., Thierry, J. C., Walker, J. E. & Wonacott, A. J. (1977). *Nature (London)*, **266**, 328–333.
Brünger, A. T., Adams, P. D., Clore, G. M., DeLano, W. L., Gros, P., Grosse-Kunstleve, R. W., Jiang, J.-S., Kuszewski, J., Nilges, M., Pannu, N. S., Read, R. J., Rice, L. M., Simonson, T. & Warren, G. L. (1998). *Acta Cryst.* D**54**, 905–921.
Cámara-Artigas, A., Hirasawa, M., Knaff, D. B., Wang, M. & Allen, J. P. (2006). *Acta Cryst.* F**62**, 1087–1092.
Cerff, R. (1979). *Eur. J. Biochem.* **94**, 243–247.
Cook, W. J., Senkovich, O. & Chattopadhyay, D. (2009). *BMC Struct. Biol.* **9**, 9.
Falini, G., Fermani, S., Ripamonti, A., Sabatino, P., Sparla, F., Pupillo, P. & Trost, P. (2003). *Biochemistry*, **42**, 4631–4639.
Fermani, S., Ripamonti, A., Sabatino, P., Zanotti, G., Scagliarini, S., Sparla, F., Trost, P. & Pupillo, P. (2001). *J. Mol. Biol.* **314**, 527–542.
Fermani, S., Sparla, F., Falini, G., Martelli, P. L., Casadio, R., Pupillo, P., Ripamonti, A. & Trost, P. (2007). *Proc. Natl Acad. Sci. USA*, **104**, 11109–11114.
Ferri, G., Stoppini, M., Meloni, M., Zapponi, M. C. & Iadarola, P. (1990). *Biochim. Biophys. Acta*, **1041**, 36–42.
Figge, R. M., Schubert, M., Brinkmann, H. & Cerff, R. (1999). *Mol. Biol. Evol.* **16**, 429–440.
Graciet, E., Gans, P., Wedel, N., Lebreton, S., Camadro, J. M. & Gontero, B. (2003). *Biochemistry*, **42**, 8163–8170.
Graciet, E., Lebreton, S., Camadro, J. M. & Gontero, B. (2003). *Eur. J. Biochem.* **270**, 129–136.
Graciet, E., Mulliert, G., Lebreton, S. & Gontero, B. (2004). *Eur. J. Biochem.* **271**, 4737–4744.
Howard, T. P., Metodiev, M., Lloyd, J. C. & Raines, C. A. (2008). *Proc. Natl Acad. Sci. USA*, **105**, 4056–4061.
Kim, H., Feil, I. K., Verlinde, C. L., Petra, P. H. & Hol, W. G. (1995). *Biochemistry*, **34**, 14975–14986.
Kissinger, C. R., Gehlhaar, D. K., Smith, B. A. & Bouzida, D. (2001). *Acta Cryst.* D**57**, 1474–1479.
Kitatani, T., Nakamura, Y., Wada, K., Kinoshita, T., Tamoi, M., Shigeoka, S. & Tada, T. (2006*a*). *Acta Cryst.* F**62**, 315–319.
Kitatani, T., Nakamura, Y., Wada, K., Kinoshita, T., Tamoi, M., Shigeoka, S. & Tada, T. (2006*b*). *Acta Cryst.* F**62**, 727–730.
Koksharova, O., Schubert, M., Shestakov, S. & Cerff, R. (1998). *Plant Mol. Biol.* **36**, 183–194.
Laskowski, R. A., MacArthur, M. W., Moss, D. S. & Thornton, J. M. (1993). *J. Appl. Cryst.* **26**, 283–291.
Luzzati, V. (1952). *Acta Cryst.* **5**, 802–810.
Marri, L., Trost, P., Pupillo, P. & Sparla, F. (2005). *Plant Physiol.* **139**, 1433–1443.
Marri, L., Trost, P., Trivelli, X., Gonnelli, L., Pupillo, P. & Sparla, F. (2008). *J. Biol. Chem.* **283**, 1831–1838.
Marri, L., Zaffagnini, M., Collin, V., Issakidis-Bourguet, E., Lemaire, S. D., Pupillo, P., Sparla, F., Miginiac-Maslow, M. & Trost, P. (2009). *Mol. Plant*, **2**, 259–269.
Matthews, B. W. (1968). *J. Mol. Biol.* **33**, 491–497.
McRee, D. E. (1999). *J. Struct. Biol.* **125**, 156–165.
Moniot, S., Bruno, S., Vonrhein, C., Didierjean, C., Boschi-Muller, S., Vas, M., Bricogne, G., Branlant, G., Mozzarelli, A. & Corbier, C. (2008). *J. Biol. Chem.* **283**, 21693–21702.
Moras, D., Olsen, K. W., Sabesan, M. N., Buehner, M., Ford, G. C. & Rossmann, M. G. (1975). *J. Biol. Chem.* **250**, 9137–9162.
Navaza, J. (1994). *Acta Cryst.* A**50**, 157–163.
Otwinowski, Z. & Minor, W. (1997). *Methods Enzymol.* **276**, 307–326.
Petersen, J., Teich, R., Becker, B., Cerff, R. & Brinkmann, H. (2006). *Mol. Biol. Evol.* **23**, 1109–1118.
Pettersen, E. F., Goddard, T. D., Huang, C. C., Couch, G. S., Greenblatt, D. M., Meng, E. C. & Ferrin, T. E. (2004). *J. Comput. Chem.* **25**, 1605–1612.
Pupillo, P. & Giuliani Piccari, G. (1975). *Eur. J. Biochem.* **51**, 475–482.
Scagliarini, S., Trost, P. & Pupillo, P. (1998). *J. Exp. Bot.* **49**, 1307–1315.
Scheibe, R., Wedel, N., Vetter, S., Emmerlich, V. & Sauermann, S. M. (2002). *Eur. J. Biochem.* **269**, 5617–5624.
Sparla, F., Fermani, S., Falini, G., Zaffagnini, M., Ripamonti, A., Sabatino, P., Pupillo, P. & Trost, P. (2004). *J. Mol. Biol.* **340**, 1025–1037.
Sparla, F., Zaffagnini, M., Wedel, N., Scheibe, R., Pupillo, P. & Trost, P. (2005). *Plant Physiol.* **138**, 2210–2216.
Tamoi, M., Ishikawa, T., Takeda, T. & Shigeoka, S. (1996). *Biochem. J.* **316**, 685–690.
Trost, P., Fermani, S., Marri, L., Zaffagnini, M., Falini, G., Scagliarini, S., Pupillo, P. & Sparla, F. (2006). *Photosynth. Res.* **89**, 263–275.
Trost, P., Scagliarini, S., Valenti, V. & Pupillo, P. (1993). *Planta*, **190**, 320–326.
Wedel, N. & Soll, J. (1998). *Proc. Natl Acad. Sci. USA*, **95**, 9699–9704.